AATCC Review

26 May 2024: Received
29 June 2024: Revised
28 July 2024: Accepted
11 September 2024: Available Online

https://aatcc.peerjournals.net/

Research Article Open Access

Assessing and Mapping of Salt Affected and Waterlogged Soils in Nagarjuna Sagar Left Bank Canal Command Area of Deccan Plateau Using the AVIRIS NG Hyperspectral Data

G Kiran Reddy[a,*], G Jayasree[a], SHK Sharma[a], TL Neelima[b], SA Hussain[b], M Triveni[c]

[a]Department of Soil Science and Agricultural Chemistry, College of Agriculture Professor Jayashanker Telangana State Agricultural University, Rajendranagar, Hyderabad- 500030, India
[b]Department of Agronomy, College of Agriculture Professor Jayashanker Telangana State Agricultural University, Rajendranagar, Hyderabad- 500030, India
[c]Department of Microbiology and Bioenergy, College of Agriculture Professor Jayashanker Telangana State Agricultural University, Rajendranagar, Hyderabad- 500030, India

ABSTRACT

By using the AVIRIS NG Hyperspectral data, analyzed the relationship between the soil spectral reflectance and various degree of salt affectedness and waterlogged soils from the soil sampling sites from Nagarjuna Sagar Left Bank Command area, Nalgonda district, Telangana, India. The individual AVIRIS NG Hyperspectral image scenes were processed with ENVI 5.3 software geocoded, and mosaicked, and the data is subjected to MNF, performed PPI, n-D visualizer, and classification (mapping) for salt-affected and waterlogged soils was attempted using the Spectral Angle Mapper algorithm. Out of the total classified area normal, slightly saline-sodic, moderately saline-sodic, severely saline-sodic, and waterlogged soils occupy 67.9, 17.0, 3.42, 7.27 and 0.04%, respectively. The Pearson correlation studies showed that 1830, 1850, 1930, 1935, and 1940 nm wavelengths significantly showed a negative correlation with EC, ESP, and CEC. The PCR model showed the possibility of retrieval of EC, ESP, and CEC more accurately. The SAM classification for AVIRIS NG showed a producer accuracy percentage of 76.4- 88.4 and a user accuracy percentage of 77.4-87.9.

Keywords: *AVIRIS NG, minimum noise fraction, pixel purity index, SAM, spectral library, ENVI, salt-affected soils, waterlogged soils*

1. Introduction

India is blessed with wealth of natural resources, but with these blessings comes the responsibility to ensure their conservation. The natural resource sectors are immensely important to India's economy. Soil is a valuable and renewable natural resource as long as it is used according to its potential. Continued unplanned and unscientific exploitation results in adverse effects on soil quality, which finally leads to land degradation. Waterlogged and salt-affected soils are the severe environmental degradation processes that impede crop growth and production [1]. Soil salinity and sodicity in arid and semi-arid environments, where crop water requirements, in addition to rainfall, are augmented by irrigation supplies, is a major concern for the sustainability of the agricultural systems [2,3]. A large area of the Nagarjuna Sagar Left Bank Command area of Nalgonda district of Telangana state consists of the irrigated command area of arid and semi-arid climatic conditions and these areas face the threat of land degradation due to salinization and alkalization in future. Therefore, the need for assessing the occurrence of soil salinization and alkalization-induced land degradation and degree of severity at any given time becomes of vital importance for agricultural sustainability in the study area.

*Corresponding Author: ***G Kiran Reddy***

DOI: https://doi.org/10.21276/AATCCReview.2024.12.03.227

The problems of salt-affected and waterlogged soils are long-standing ones, but their area and intensity have been increasing at alarming rates mainly because of poor water quality, poor on-farm water management practices, and lack of adequate drainage facilities in fields. Waterlogging and accumulation (both salinity and sodicity) are the two main problems in the irrigated ecosystems of command areas of arid and semi-arid regions. Salinity and alkalinity are the root causes that lead to land deterioration in these regions [4]. This has resulted in vast stretches of wasteland and a reduction in arable land, which is the product of a complex interaction of many variables, it lessens the current and/or potential capability of soil to produce goods and services. Arid and semi-arid regions are under high pressure to supply the required food for their rapidly increasing populations. The consequent changes in land use mainly due to the common policy of agricultural intensification, together with the harsh climatic conditions, have accelerated the above - mentioned problems. It reduces the soil quality, limits the choice of crops to be grown, major limiting factor for reduced yields, and in extreme cases, it leads to the abandonment of agricultural lands [5,6].

Salt-affected and waterlogged soils are not as controversial as other environmental issues like global warming, climate change, water pollution, water scarcity, air pollution, and deforestation. But it should not be underestimated. It is understood that if salt-affected soils increase in the future at present rate, a lot of countries will suffer from producing enough food for their growing population [7]. The current study focussed on differentiating salt-affected soils and non-salt-affected soils, qualitatively zand analyzing the distribution of

salt-affected soils and monitoring.

In the recent past, there has been a growing interest in identifying rapid and less expensive tools for salt-affected and waterlogged soil assessment worldwide because characterization, mapping, and monitoring of salt-affected soils and waterlogged soils by the ground survey is difficult as the salt concentration may vary substantially over short distances and time-consuming [8]. Remote sensed data and GIS are of great advantage in the assessment of salt-affected soils, they help in assessment in less time, and distribution will be known in less time [9,10,11] which is of utmost importance both from the agricultural and environmental perspectives.

AVIRIS NG Hyperspectral remote sensing data in the form of imaging spectrometer data provide high spatial resolution data in a large number of narrow contiguous spectral bands in the VNIR - SWIR region (380 to 2510 nm) [12]. Using hyperspectral remote sensing data continuous response curves of target features in the visible, near-infrared (NIR), and shortwave infrared (SWIR) wavelengths can be generated. This continuous spectral response curve is referred to as the spectral signature. As it acquires data in many narrow wavelength bands, it allows the use of almost continuous data in studying the Earth's surface. This produces laboratory-like reflectance spectra with absorption bands specific to object properties and also increases the accuracy of mapping.

AVIRIS NG hyperspectral remote sensing is a rapid, versatile, reliable, and powerful tool for knowing the salt-affected and waterlogged soils because of the high spectral resolution (<5 nm) and this narrow band can discriminate the critical spectral differentials in detail compared to board band sensors (>50 nm) which may lose the important spectral information [13].

With this background, the present study "Assessing and Mapping of Salt Affected and Waterlogged Soils in Nagarjuna Sagar Left Bank Command Area of Deccan Plateau using the AVIRIS NG Hyperspectral Data" is taken up.

2. Methods and materials

2.1. Location of study area

The study area was a part of Nalgonda district, Telangana, India, and lies between the 16.9315 N 79.2784 E and 16.9144 N 79.7194 E in Southern Telangana Zone (Figure 1). The study area was characterized by semi-arid climatic conditions, with an average rainfall of 788.5 mm of which 86 percent was received during the southwest monsoon, 5 percent during the northeast monsoon and 9 percent during the summer season. Mean monthly rainfall was the highest in September followed by August, July, June, October, and May. The mean relative humidity for forenoon and afternoon are 78.9 percent and 46.8 percent, respectively. The mean monthly relative humidity was the highest in September (91 percent) and the lowest in January (28 percent). The mean monthly temperature ranges from 14.0 °C to 40 °C. The minimum temperature was recorded during December (13.0 °C) and maximum in May (39.0 °C). The maximum temperature remains between 30.3 °C to 35.5 °C during July to December. In Nalgonda, the wet season was oppressive and overcast, the dry season was humid and mostly clear, and it was hot year-round. Over the course of the year, the temperature typically varies from 17.2 °C to 40 °C and is rarely below 14.4 °C or above 43.3 °C. The soils are comprised of red, black, alkaline, and alluvium soil. The red and black soil constitutes most of the area. Black soil was found over the limestone area.

2.2. Satellite Data Used

The Airborne Visible and Infra-Red Imaging Spectrometer – Next Generation (AVIRIS-NG) is a push-broom imaging spectrometer of the Jet Propulsion Laboratory (JPL), NASA – Level 2 reflectance data has been used for the present investigation. It is part of the joint operation of the ISRO-NASA airborne campaign and onboard an ISRO B200 aircraft. There are 425 narrow continuous spectral bands in VNIR and SWIR regions in the range of 380- 2510 nm at 5 nm band interval with high SNR (>2000 @ 600 nm and >1000 @ 2200 nm) with an accuracy of 95 percent having FOV of 34 deg and IFOV of 1 mrad. Ground Sampling Distance (GSD) vis-a-vis pixel resolution varied from 4 to 8 m for a flight altitude of 4-8 km for a swath of 4-6 km [12]. Data was acquired with a resolution of 5 m. The huge data had an enormous amount of information [14], but the data had noisy bands. The noisy bands are the result of various absorptions like water vapor, oxygen, and CO_2 absorption regions [15] which were removed prior to data dimensionality reduction. After locating the presence of similar spectral information over certain contiguous ranges, bands were found suitable and used for this study. The AVIRIS-NG campaign was conducted in the region in a total of seven scenes in the study area.

2.3. AVIRIS NG data processing and methodology (Figure 2)

A total of seven AVIRIS NG level 2 reflectance scenes have been acquired and patched to prepare the seamless mosaic image of the study area by using the EVNI 5.3 software for the analysis of the digital image. Vigorous processing and analysis of satellite imageries were performed for better analysis and interpretation of datasets for mapping salt-affected and waterlogged soils. It included bad band removal, destripping, and reduction of noise pixels. Out of the 425 bands of AVIRIS NG hyperspectral data, some of the bands were not illuminated and others corresponded to areas of low sensitivity and were in the lower and upper ends of the spectral range exhibiting poor signal-to-to-to-noise ratio, so the spectral subset was done and removed the unwanted bands. The spectral subset was performed to remove bad bands that resulted in continuous spectra from the image. After the removal of bad bands, 287 good bands remained for further processing [16]. The bad columns that had relatively different values as compared to the surrounding values were repaired. This was done by taking an average of preceding and succeeding values on either side of the bad column. Bad pixels or random noise was reduced by running the convolution filter over the image. Visual examination and iscomparison of bands in raw AVIRIS NG Hyperspectral data and preprocessed data have resulted in noise-reduced images.

MNF transformation was used to reduce the dimensionality of the hyperspectral dataset by segregating the noise in the data and to reduce the computational requirements for subsequent processing [17]. The MNF was a linear transformation which was essentially a two-cascaded principal component analysis (PCA) transformation. After applying the MNF technique on the 287 good bands, new 287 MNF bands were generated. The image pixels were represented by eigenvalues and the dimensionality of the data was determined by examining these values. When examining these values, it was observed that the first 23 bands had the highest eigenvalues (>4) while the rest had values less than 4 which don't provide any information (Figures 3 and 4). These low values were seen in the image as noise. It was seen that noise was segregated in the higher number MNF bands and it was noted that there was a decrease in spatial coherency with increasing MNF band number.

So the first 23 bands of the MNF transformation were selected for further processing [18,19,20].

The PPI (Pixel Purity Index) was a means of finding the most "spectrally pure" or extreme pixels in the multispectral and hyperspectral images [21]. The most spectrally pure pixels typically correspond to mixing endmembers. The Pixel Purity Index was computed by repeatedly projecting n-dimensional scatter plots onto a random unit vector. The extreme pixels in each projection were recorded and the total number of times each pixel was marked as extreme was noted. A "Pixel Purity Image" was created in which the digital numbers in each pixel correspond to the number of times that pixel was recorded as extreme. The PPI was run on an MNF transform result excluding the noise bands [22]. The spectra can be thought of as points in dimensional space, where n was the number of bands. Five endmembers namely normal soil, slight, moderate, severely saline-sodic, and waterlogged soils were extracted for the further classification of the image [23].

2.4. Mapping Method

Salt-affected and waterlogged soils standard spectra were generated by taking the average soil spectra from various salt-affected and waterlogged soils using the reflectance collected from the soil sampling site and they were used to develop the spectral library of individual salt-affected and waterlogged soils and by using the developed spectral library, AVIRIS NG image is classified by using the algorithm SAM (spectral angle mapper).

2.5. Soil Sample Collection, Analysis and Characterization

Random sampling technique was applied and a total of 102 Global Positioning System (GPS) based soil samples of 0-30 cm depth were collected from the study area based soil variation using satellite image RS 2 (LISS-III and LISS-IV). Soil samples collected were dried under shade. The air-dried samples were pounded using a wooden pestle and mortar passed through 2 mm sieve and stored for determination of various soil properties.

pH of the soil samples was determined in 1:2.5 soil water suspension by using a pH meter (DI-707) with a glass electrode [24]. The electrical conductivity was determined in 1:2.5 soil water extract with the help of a digital conductivity meter (DI-909) and results were expressed in dS m^{-1} [24]. The sodium (Na^+) concentration of the soil extracts was measured by a flame photometer [24]. The CEC of the soils was determined by Bower et al. (1952) [25] by estimating the concentration of the sodium in the leachate by aspirating directly into a flame photometer expressed as c mol [p^+] kg^{-1} soil.

The exchangeable sodium percentage (ESP) of the soil samples was calculated using the formula

ESP = (Exchangeable Na^+ / CEC) x 100

Based on the characterization of the soils of the study area they were grouped into five endmembers namely normal, slightly saline-sodic, moderately saline-sodic, severely saline-sodic, and waterlogged classes. The categorization of salt-affected soil was adopted from the Project manual NRC Land Degradation Mapping using multi-temporal satellite data NRSC 2007 and given in table 1. Waterlogged soils were characterized by visual interpretation.

2.6. Instruments and software used

GPS was used to obtain the geographical coordinates of the observed field locations during the ground truth study for collecting soil and land use/land cover information. Soil samples were collected from 0 – 30 cm depth from the study area. ENVI (version 5.3) and ERDAS IMAGINE (version 9.1) software were used to process and classify AVIRIS NG data.

2.7. Statistical analysis

Pearson product-moment correlation coefficient was used to measure the degree of the linear relationship between the measured soil variables with reflectance values as well as absorption feature parameter at obtained wavelength intervals characteristics of a certain soil parameter by using SPSS window version 17.0 (SPSS Inc., Chicago, USA) and MMicrosoft office (version 2010). The PCR algorithm has inferential capability, which was used to model a possible linear relationship.

2.8 Accuracy assessment

Accuracy assessment was carried out in ENVI IMAGINE by comparing the classification product (containing various salt-affected and waterlogged soil classes) with recorded field observation (ground truth) which was believed to reflect the true salt-affected and waterlogged soil classes accurately. The producers, users, and kappa coefficient were estimated.

3. Results and discussion

3.1. Characterisation of salt-affected and waterlogged soils

The surface soil samples were zanalyzed for pH, EC, Exchangeable Na^+, ESP, and CEC, and soils were grouped into normal, slightly saline-sodic, moderately saline-sodic, severely saline-sodic, and waterlogged soils (Table 2) considering EC and ESP values of the collected soil samples. The pH of the normal soils ranged from 6.78 to 9.04, slightly saline-sodic from 6.12 to 9.62, moderately saline-sodic from 6.78 to 8.22, severely saline-sodic from 7.23 to 9.23, and waterlogged soils from 6.98 to 9.01. From the results, it was observed that the soil reaction of the study area ranged from neutral to alkaline in nature. The EC values varied from 0.19 to 4.33 dS m^{-1}, which indicates that EC values in the study area are at various stages of salinity in the collected soil samples. The EC values (dS m^{-1}) of the normal soils ranged from 0.19 to 1.98, slightly saline-sodic from 0.35 to 3.96, moderately saline-sodic from 0.17 to 3.98, severely saline-sodic from 2.95 to 4.33 and waterlogged soils from 0.29 to 3.89. In some of the locations, soil showed extreme salinity levels whereas some of the areas contained normal soil with no salinity hazard. On average, the studied area represented marginally saline to saline types of soil. The exchangeable Na^+ values of the samples collected from the study area varied greatly and ranged from 0.23 to 15.4 c mol (p^+) kg^{-1}, which indicates various stages of sodicity in the study area. Results revealed that the exchangeable Na^+ values varied from 0.23–1.58, 0.96–3.10, 1.43–6.01, 4.91–15.4, and 0.33–7.89 c mol (p^+) kg^{-1}, respectively, for normal soils, slightly saline-sodic, moderately saline-sodic, severely saline-sodic and waterlogged soils. Results revealed that the ESP values of the soil samples collected from the study area ranged from 1.35 to 41.96 which indicates the influence of sodium hazard in such soil in some of the pockets which were mostly saline-sodic in nature. The soil ESP (percent) ranged from 1.35 to 5.14 for normal soils, 5.20 to 9.69 for slightly saline-sodic soils, 5.96 to 19.62 for moderately saline-sodic soils, 22.39 to 41.96 for severely saline-sodic soils and 1.64 to 25.25 in waterlogged soils. The soil CEC ranged from 15.10 to 37.10 c mol (p^+) kg^{-1}. The result revealed that the CEC values varied from 15.10-35.00, 18.00-33.20, 19.10-34.50, 19.00-37.10, and 18.10-34.25 c mol (p^+) kg^{-1}, respectively, for normal soils, slightly saline-sodic, moderately saline-sodic, severely saline-sodic and waterlogged soils.

3.2. Spectral Features

102 soil samples were classified into five classes based on the varying degree of salt affectedness and waterlogged soil. The spectra of each identified class were averaged as representative spectra. Five spectra extracted from endmembers have followed a similar basic trend and there were two obvious absorption features at 1480 and 1980 nm. Figure 5 shows the reflectance spectra of saline-sodic and waterlogged soils. In general, the reflectance increased across the spectrum with increasing severity of salinity. A similar observation was reported by [26]. The pH, EC, and as well as ESP increased compared to normal soil (Table 2). A perusal of spectra also revealed that although there was a steady increase in reflectance for all the soil samples with the increase in electromagnetic wavelength, a significant decrease in reflectance at 1480 and 1980 nm was observed, which was most prominent in all 3 categories viz., severely saline-sodic, moderately saline-sodic and slightly saline-sodic soils. A significant decrease in reflectance at 1480 and 1980 nm wavelength was observed irrespective of soil samples because of higher absorption due to the presence of moisture and hydroxyl ions. The more prominent absorption dips were found in sodic soil because of the fact it contains the anions such as chloride, sulfate, and carbonates to a great extent which were hygroscopic in nature as well as abundant quantities of Mg^{+2} and Na^{+} cations having higher hydration energy which can hold more water. It was also observed that the salt-affected soils exhibited comparatively higher reflectance values throughout the entire wavelengths (380–2510 nm) compared to normal and waterlogged soil samples. [27,28,29] have also reported higher reflectance values in salt-affected soils than in normal soil in the entire wavelength range. Severely saline-sodic soils showed very high reflectance throughout the spectrum compared to other soils. But severely and moderately saline-sodic soils showed a reflectance dip at 1870 and 1980 nm than slightly saline-sodic soils. Waterlogged soils showed much lower soil spectral reflectance values compared to normal, slightly, moderately, and severely saline-sodic soils because of the presence of a greater amount of moisture in the soil samples during the spectral measurements. As the moisture content in soil increases, the spectral reflectance decreases as it absorbs much radiation beyond visible wavelength. Similar findings were reported by [30,31,32].

3.3. Classification of AVIRIS NG Hyperspectral Data for salt-affected and waterlogged soil

The spatial distribution of different salt-affected and waterlogged soils of the study area was mapped using the SAM algorithm. The final classification result is shown in Figure 6. Study area SAM classified image revealed that extensive areas were classified as normal soil comprising around 67.99 percent of the total classified area followed by slightly saline-sodic soils occupying 17.01 percent of the total classified area. About 7.27 percent area was severely saline-sodic soil in the study. Results showed that moderately saline-sodic soils distributed only 3.42 percent of the total classified area. Waterlogged soils comprised around 4.32 per cent of the total classified area. The non-agricultural land, water bodies, roads, forest vegetation, and builtup area in the study area coincide with unclassified pixels [33,34,35,36,37].

3.4. Accuracy Assessment

An accuracy assessment was carried out in order to know how accurately pixels were classified into different classes of salt-affected and waterlogged soils.

Each of the pixels was computed and analyzed for the producer's, and user's accuracy as well as the kappa coefficient. Results of Nagarjuna Sagar Left Bank Command area revealed that among the salt-affected soil classes normal soil showed 85.0 percent user accuracy followed by severely saline-sodic soil (82.3 percent), moderately saline-sodic soil (78.2 percent) and slightly saline soil (77.4 percent). Waterlogged soils showed 87.9 percent user accuracy (Table 3) [33,38] AVIRIS NG data as showed the higher accuracy [39].

3.5. Soil properties VS reflectance behavior in AVIRIS NG Hyperspectral Data

To understand the influence of the soil properties on the spectral reflectance curve, correlation studies were carried out with resampled reflectance values at 5-nm intervals for the entire waveband. The Pearson correlation matrix was given in Table 4.

The results observed were in conformity with the study of [40] which showed that EC, ESP, and CEC had significant correlation with reflectance for 745, 755, 760, 765, 775, 780, and 810 nm wavelength. The soil properties like EC, CEC, and ESP showed significant negative correlation at 1830 nm (r= -0.380*, - 0.224* and -0.403*) wavelength, 1850 nm (r= -0.338*, -0.309*, -0.475* and -0.403*) wavelength, 1930 nm (r= -0.322*, -0.307* and -0.338*) wavelength, 1935nm (r= -0.376*, -0.312* and -0.404*) wavelength and 1940 nm (r= -0.540*, -0.309* and -0.478*) wavelength.

3.6. Prediction of soil properties using Principal Component Regression (PCR) analysis

The results obtained based on the PCR model showed that good predictions of soil properties can be made more accurately and in line with [41] and [42]. The equations derived from the PCR analysis for soil properties are presented in Table 5. The results showed that soil parameters EC, ESP, and CEC predictions can be made accurately based on PCR model values (R^2) of such soil properties showed a somewhat reasonable correlation under study (Table 5).

The R^2 values of predicted parameter vs observed parameter for EC, CEC, and ESP were 0.663, 0.490, and 0.341 respectively as depicted in Figures 7a, b, and c, and RMSE values of 1.212, 6.448, and 3.389 respectively (Kumar et al. 2015).

4. Conclusion

The spectral characteristics of the different salt-affectedness and waterlogged soils tend to be consistent. But as the degree of salt-affected soils increases the spectral reflectance increases. The reflectance spectra were generated using AVIRIS NG Hyperspectral images covering a range of 380-2510 nm. An increasing trend of soil reflectance with an increase in wavelength of electromagnetic radiation was observed irrespective of the nature of the soils. A significant decrease in reflectance at 1480 and 1980 nm wavelength was observed which is more prominent in severely saline-sodic soils. It is also observed that saline soils exhibited comparatively much higher reflectance values throughout the wavelength (380-2510) compared to normal soil samples and their similarity was measured using SAM. Study area under normal soils was found to be 67.99 percent, the slightly saline-sodic category was 17.01 percent, the moderately saline-sodic category was 3.42 percent, severely saline-sodic soils was 7.27 percent, and the area under waterlogged soils was 4.32 percent of the classified area. The Pearson correlation studies were carried out with resampled reflectance values at 5 nm intervals for the entire wavelength range.

The soil properties like EC, Mg, CEC, and ESP showed significant negative correlation strongly at 1830, 1850, 1930, 1935, and 1940 nm wavelengths. The PCR was used to model the correlation between soil reflectance spectra (Predictor variables) and soil physic-chemical properties of salt-affected soil (response variable). Prediction models were developed for soil properties. The PCR model showed the possibility of retrieval of EC, ESP, and CEC more accurately.

Declaration of Competing Interest: None

Acknowledgment: I am highly thankful to AVIRIS NG Project, SAC, Ahmadabad for sharing the Hyperspectral data.

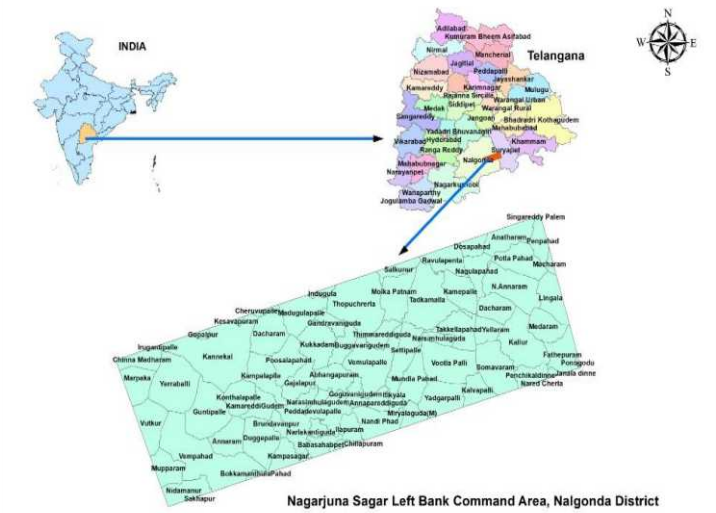

Figure 1: Study area of Nagarjuna Sagar Left Bank Command area, Nalgonda district

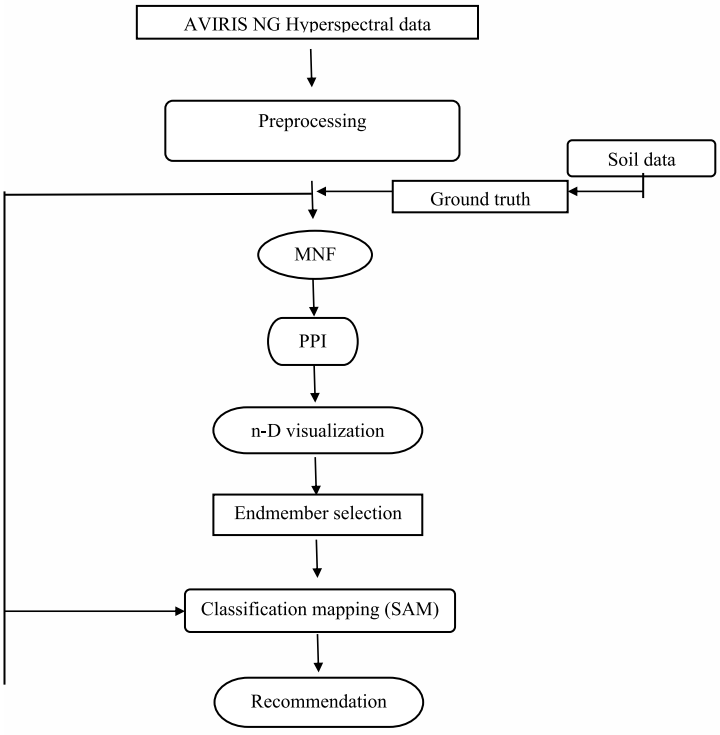

Figure 2. Flow diagram for methodology of processing of AVIRIS NG Hyperspectral data

Bands	Eigenvalues
1.000000	723.831384
2.000000	90.622303
3.000000	43.811863
4.000000	29.346210
5.000000	21.867898
6.000000	18.635627
7.000000	14.789189
8.000000	14.192412
9.000000	12.730552
10.000000	11.883526
11.000000	10.763558
12.000000	10.040314
13.000000	9.416699
14.000000	8.579446
15.000000	8.230108
16.000000	6.858113
17.000000	6.791340
18.000000	6.317949
19.000000	5.754824
20.000000	5.568841
21.000000	4.754586
22.000000	4.558610
23.000000	4.474659

Figure 3: MNF transformed data Eigen values in Nagarjuna Sagar Left Bank Command area from AVIRIS NG Hyperspectral image

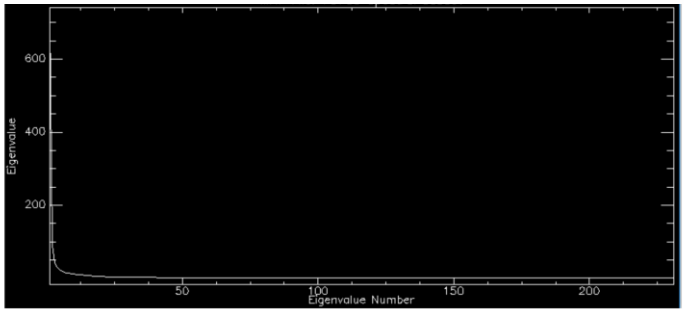

Figure 4: MNF Eigen values plot in Nagarjuna Sagar Left Bank Command area from AVIRIS NG Hyperspectral image

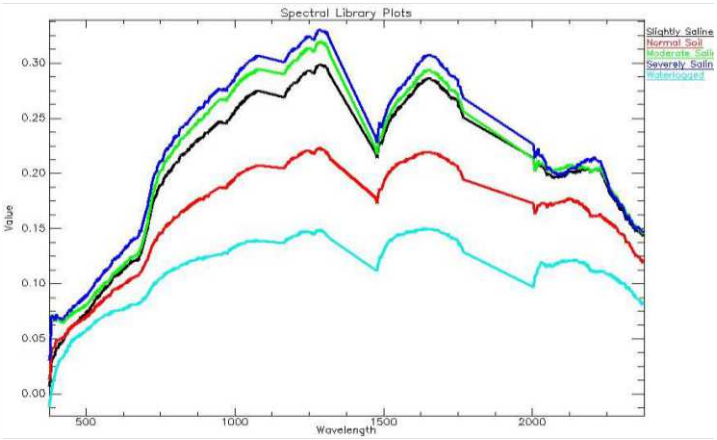

Figure 5: Spectral profile of salt affected and waterlogged soils from AVIRIS NG Hyperspectral data of Nagarjuna Sagar Left Bank Canal Command area (Dark Blue – Severe saline sodic, Green – Moderately saline sodic, Black – Slightly saline sodic, Red – Normal soils and Blue – Waterlogged soils)

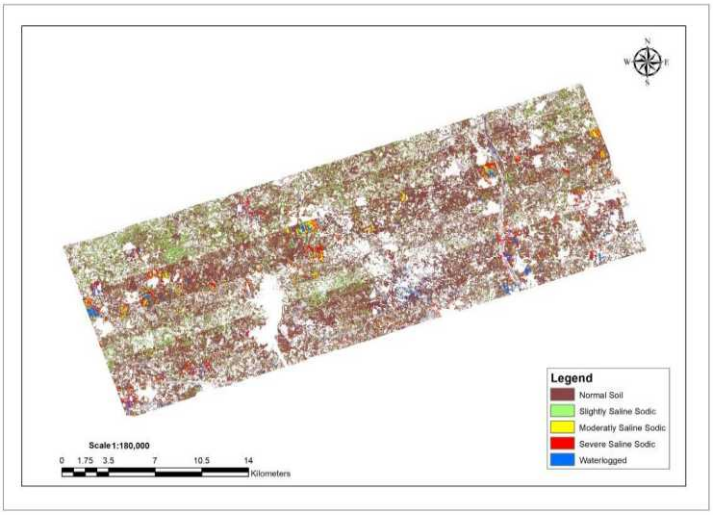

Figure 6: Spectral Angle Mapper classified image of salt affected and waterlogged soils in Nagarjuna Sagar Left Bank Command area

Figure 7: Predicted parameters vs observed parameters in PCR model

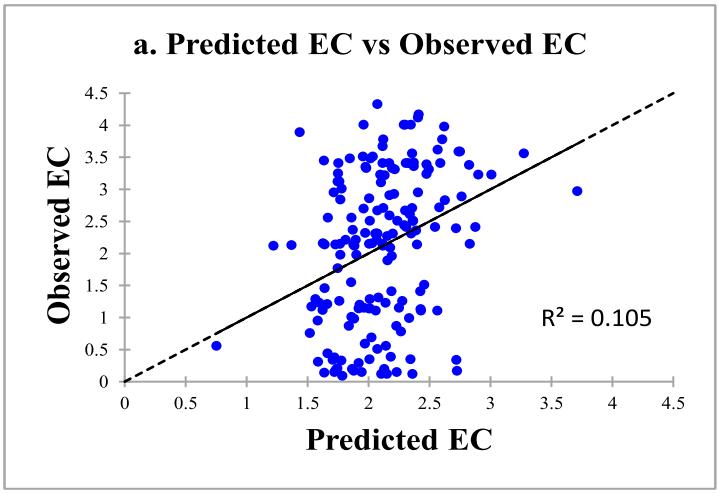

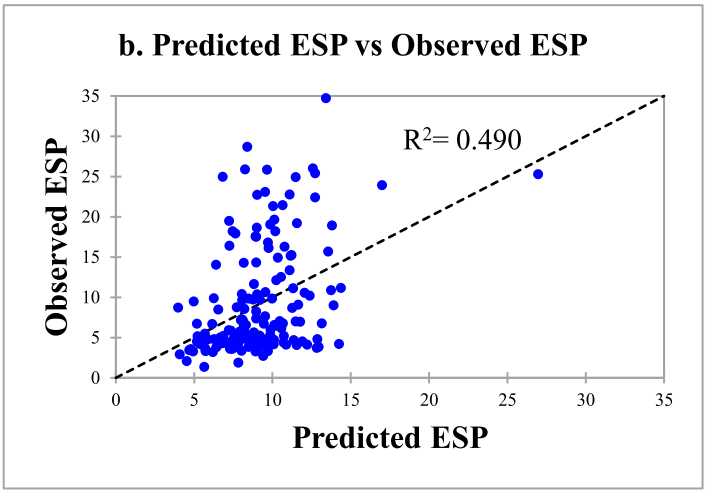

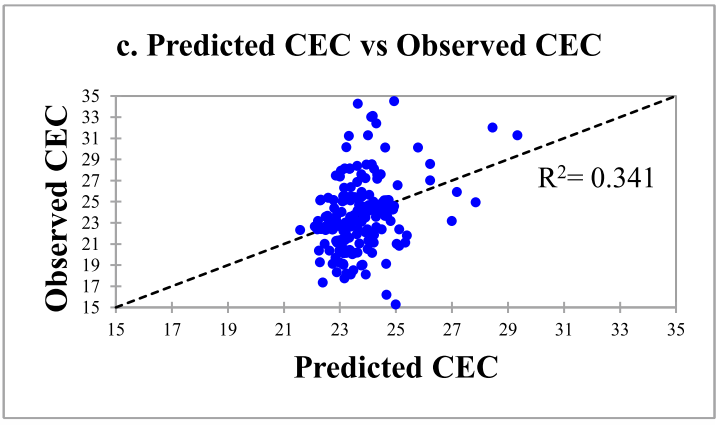

Table 1: Criteria for assessing salt affected soil in black/non black soil

S. No.	Class	Salinity (dS m^{-1})		ESP	
		Black soil	Other soil	Black soil	Other soil
1	Slight	2-4	4-8	5-10	15-40
2	Moderate	4-8	8-16	10-20	40-60
3	Severe	>8	>16	>20	>60

S. No.	Type	Class included		
		Slight	Moderate	Severe
1	Saline	S1	S2	S3
2	Sodic	N1	N2	N3
3	Saline-Sodic	S1N1	S1N2, S2N1, S2N2	S1N3,S2N3,S3N1, S3N2, S3N3

(Source: Project manual NRC-Land degradation mapping using multi temporal satellite data, NRSC 2007)
Note: S = Saline: N = Sodic : SN = Saline – sodic

Table 2: Ranges of soil properties for the identified salt affected and waterlogged soil class of Nagarjuna Sagar Left Bank Command Area, Nalgonda district

	pH	EC (dS m^{-1})	Exch. Na^+ (c mol $[p^+]$ kg^{-1})	CEC (c mol [p+] kg^{-1})	ESP
Normal Soils					
Mean	7.81	0.99	0.91	24.60	3.65
Range	6.8-9.0	0.2-2.0	0.2-1.6	15.1-35.0	1.4-5.1
SD	0.45	0.51	0.29	4.74	0.89
Slightly saline-sodic soils					
Mean	8.08	2.94	1.96	25.63	7.50
Range	6.1-9.62	0.4-4.0	1.0-3.1	18.0-33.2	5.2-9.7
SD	0.79	0.85	0.65	4.80	1.58
Moderately saline-sodic soils					
Mean	7.73	3.03	3.46	24.41	13.99
Range	6.8-8.2	0.2-4.0	1.4-6.0	19.1-34.5	6.0-19.6
SD	0.50	1.22	1.44	5.47	4.24
Severely saline-sodic soils					
Mean	8.34	3.45	8.52	27.26	30.4
Range	7.2-9.2	3.0-4.3	4.9-15.4	19.0-37.1	22.4-42.0
SD	0.56	0.39	3.51	6.29	6.33
Waterlogged soils					
Mean	8.17	2.64	2.89	25.08	10.45
Range	7.0-9.0	0.3-3.9	0.3-7.9	18.1-34.2	1.6-25.2
SD	0.67	1.26	2.49	5.68	7.30

Table 3: Accuracy assessment of the classified salt affected and waterlogged soil map of Nagarjuna Sagar Left Bank Canal Command area, Nalgonda district from AVIRIS NG Hyperspectral data

Category	Producer's accuracy (per cent)	User's accuracy (per cent)	Kappa coefficient
Normal soils	88.4	85.0	0.85
Slightly Saline Sodic soils	76.4	77.4	0.76
Moderately Saline Sodic soils	77.5	78.2	0.78
Severely Saline Sodic soils	81.2	82.3	0.81
Waterlogged soils	87.3	87.9	0.88

Table 4: Correlation matrix of EC, CEC and ESP with 425 bands of spectral reflectance

Band	EC	CEC	ESP
745	0.143*	0.221**	0.252**
750	0.142	0.222**	0.250**
755	0.143*	0.224**	0.251**
760	0.146*	0.224**	0.251**
765	0.149*	0.224**	0.244**
770	0.125	0.222**	0.249**
775	0.149*	0.223**	0.251**
780	0.144*	0.220**	0.246**
785	0.142	0.219**	0.244**
790	0.142*	0.218**	0.244**
795	0.121	0.217**	0.241**
800	0.121	0.214**	0.241**
805	0.143*	0.213**	0.240**
810	0.142	0.212**	0.239**
815	0.141	0.213**	0.238**
1830	-0.380*	-0.224*	-0.403*
1835	-0.030	0.007	0.016
1840	0.057	-0.125	0.080
1845	0.098	-0.060	0.203**
1850	-0.338*	-0.309*	-0.475*
1855	0.144	-0.023	0.243**
1920	0.064	0.052	0.085
1925	-0.007	0.110	-0.020
1930	-0.322*	-0.307*	-0.338*
1935	-0.376*	-0.312*	-0.404*
1940	-0.540*	-0.309*	-0.478*
1945	-0.082	0.021	-0.017

Table 5: Predication equations for relating soil properties from reflectance spectra

Parameter	Unit	RMSE	R^2	Equation
EC	dS m^{-1}	1.212	0.663	= 4.07-620.44*B96 +21.21*B425
ESP	per cent	6.448	0.490	= 5.90+2505.14*B13-2197.54*B71+2456.41*B74
CEC	c mol $(p^+)kg^{-1}$	3.389	0.341	= 21.92-1743.98*B39+2056.39*B41-1460.04*B84

References

1. Shahbaz, M. and Ashraf, M. Improving Salinity Tolerance in Cereals. Critical Reviews in Plant Science. 2013. 32; 237-249.

2. Singh, R.P., Setia, R., Verma, V.K., Arora, S.K., Kumar, P and Pateriya, B. 2017. Satellite remote sensing of salt-affected soils: Potential and limitations. Journal of Soil and Water Conservation. 16(2): 97-107. DOI: 10.5958/2455-7145.2017.00015.7

3. Ma, Z.Q., Xu, Y.P., Peng, J., Chen, Q.X., Wan, D., He, K., Shi, Z., Li, H.Y. 2018. Spatial and temporal precipitation patterns characterized by TRMM TMPA over the Qinghai Tibetan plateau and surroundings. Int. J. Remote Sens. 39, 3891–3907.

4. Neto, O.C.D.R., Teixeira, A.D.S., Leao, R.A.D.O., Moreira, L.C.J and Galvao, L.S. 2017. Hyperspectral Remote Sensing for Detecting Soil Salinization Using ProSpecTIR-VS Aerial Imagery and Sensor Simulation. Remote Sensing. 9:42, doi:10.3390/rs9010042

5. Patel, R., Prasher, S., Bonnell, R and Boughton, R. 2002. Development of comprehensive soil salinity index. Journal of Irrigation and Drainage Engineering-ASCE. 128: 185-188.

6. Amezketa, E. 2006. An integrated methodology for assessing soil salinisation, a precondition for land desertification. Journal of Arid Environments. 67: 594-599.

7. Gorji, T., Yildirim, A., Hamzehpour, N., Tanik, A and Sertel, E. 2020. Soil salinity analysis of Urmia Lake Basin using Landsat-8 OLI and Sentinel2A based spectral indices and electrical conductivity measurements. Ecological Indicators. 112: 106173.

8. Kumar, N., Singh, S.K., Reddy, G.P.O. Mishra, V.N. and Bajpai, R.K. 2021. Remote Sensing Applications in Mapping Salt Affected Soils. Agricultural Reviews. 10.18805/ag.R-2008

9. Metternicht, G. I and Zinck, J. A. 2003. Remote sensing of soil salinity: Potentials and constraints. Remote Sensing of Environment. 85(1): 1–20.

10. Ennaji, W., Barakat, A., Karaoui, I., Baghdadi, M.E and Arioua, A. 2018. Remote sensing approach to assess salt-affected soils in the north-east part of Tadla plain, Morocco. Geology, Ecology, and Landscapes. 2:1, 22-28, 10.1080/24749508.2018.1438744

11. Abd El-Hamid, H.T and Hong, G. 2020. Hyperspectral remote sensing for extraction of soil salinization in the northern region of Ningxia. *Modeling Earth Systems and Environment.* 6:2487–2493, https://doi.org/10.1007/s40808-020-00829-3

12. Bhattacharya, B. K and Singh, C. P. 2017. Spectrum of India, ISRO, Ahmedabad. ISBN No.: 9789382760290

13. Bhattacharya, B.K. 2016. AVIRIS Programme and Science Plan, February. 18-22.

14. Hong, G and Abd El-Hamid, H.T. 2020. Hyperspectral imaging using multivariate analysis for simulation and prediction of agricultural crops in Ningxia,China. Comput Electron Agric J. 172:105355. https://doi.org/10.1016/j.compag.2020.105355

15. Gao, B.C., Montes, M.J., Davis, C.O and Goetz, A.F. 2009. Atmospheric correction algorithms for hyperspectral remote sensing data of land and ocean. *Remote Sensing of Environment*. 113: 17-24.

16. Govil, H., Gill, N., Rajendran, S., Santosh, M and Kumar, S. 2018. Identification of new base metal minerlization in Kumaon Himalaya, India, using hyperspectral remote sensing and hydrothermal alteration. Ore geology reviews. 92: 271-283.

17. Boardman, J.W and Kruse, F.A. 1994. Automated spectral analysis: A geologic example using AVIRIS data, north Grapevine Mountains, Nevada. In Proceedings, Tenth Thematic Conference on Geologic Remote Sensing, Environmental Research Institute of Michigan: 407-418.

18. Vibhute, A.D., Karbhari, V.K., Rajesh, K., Dhumal, L., Ajay, D.N and Suresh, C.M. 2018. Identification, classification and mapping of surface soil types using Hyperspectral Remote Sensing datasets. International Journal of Scientific Research in Computer Science, Engineering and Information Technology. 3 (1): 2456-3307.

19. Mishra, S., Chattoraj, L.S., Benny, A., Sharma, R.U and Ray, P.K.C. 2019. AVIRIS-NG data for geological applications in south-eastern parts of Aravalli Fold Belt, Rajasthan. Proceedings. 24 (16): 1-7. doi:10.3390/IECG2019-06212

20. Jain, R and Sharma, R.U. 2019. Airborne hyperspectral data for mineral mapping in south eastern Rajasthan, India. International Journal of Applied Earth Observation and Geoinformation. 81: 137-145.

21. Boardman, J.W., Kruse, F.A and Green, R.O. 1995. Mapping target signatures via partial unmixing of AVIRIS data. In summaries, fifth JPL Airborne Earth Science Workshop, JPL Publication, 1: 23-26.

22. IIRS Practical manual. 2019. Hyperspectral Remote Sensing and its application. Indian Institute of Remote Sensing, Dehradun.

23. Mishra, S., Chattoraj, L.S., Benny, A., Sharma, R.U and Ray, P.K.C. 2019. AVIRIS-NG data for geological applications in south-eastern parts of Aravalli Fold Belt, Rajasthan. Proceedings. 24 (16): 1-7. doi:10.3390/IECG2019-06212

24. Jackson, M.L. 1973. Soil Chemical Analysis. Oxford IBH Publishing House, Bombay. 38.

25. Bower, C.A., Reitemeier, R.F and Fireman, M. 1952. Exchangeable cations analysis of saline and alkali soils. *Soil Science*. 73: 251-261.

26. Wang, J and Li, X. 2020. Comparison on quantitative inversion of characteristic ions in salinized soils with hyperspectral based on support vector regression and partial least squares regression. European Journal of Remote Sensing. 53 (1): 340-348. doi: 10.1080/22797254.2020.1854622

27. Stoner, F.R. 1979. Physico-chemical, site and bidirectional reflectance factor characteristics of uniformly moist soils. Ph.D. dissertation, Purdue University, West Lafayette, Indiana.

28. Rao, B. R. M., Dwivedi, R. S., Venkataratnam, L., Ravishanker, T., Thammappa, S. S., & Bhargava, G. P. 1991. Mapping the magnitude of Sodicity in part of the Indo-Gangetic plains of Uttar Pradesh, Northern India using Landsat-TM data. International Journal of Remote Sensing.12(3): 419– 425.

29. Wang, J., Dinga, j., Yuc, D., Maa, X., Zhanga, Z., Gea, X., Tenga, D., Lia, X., Lianga, J., Lizagae, I., Chena, X., Yuanf, L and Guog, Y. 2019. Capability of Sentinel-2 MSI data for monitoring and mapping of soil salinity in dry and wet seasons in the Ebinur Lake region, Xinjiang, China. Geoderma. 353: 172-187.

30. Mandal, A.K and Sharma, R.C. 2011. Delineation and characterization of waterlogged salt affected soils in IGNP using remote sensing and GIS. Journal of the Indian Society of Remote Sensing. 39 (1): 39-50.

31. Lobell, D and Asner, G., 2002. Moisture effects on soil reflectance. Soil Sci. Soc. Am. J. 66, 722–727.

32. Fabre, S., Briottet, X and Lesaignoux, A. 2015. Estimation of soil moisture content from the spectral reflectance of bare soils in the 0.4-2.5 µm domain. *Sensors*. 15: 3262-3281. doi:10.3390/s150203262

33. Mitran, T., Ravisankar, T., Fyzee, M.A., Suresh, J.R., Sujatha, G and Sreenivas, K. 2015. Retrieval of soil physic-chemical properties towards assessing salt-affected soils using hyperspectral data. Geocarto International. 30(6): 701-721.

34. George, J and Kumar, S. 2015. Hyperspectral remote sensing in characterizing soil salinity severity using SVM technique - A case study of alluvial plains. *International Journal of Advanced Remote Sensing and GIS*. 4 (1): 1344-1360.

35. Hamzeh, S., Naseri, A.A., Alavipanah, S.K., Bartholomeus, H.M and Herold, M. 2016. Assessing the accuracy of hyperspectral and multispectral satellite imagery for categorical and quantitative mapping of salinity stress in sugarcane fields. International Journal of Applied Earth Observation and Geoinformation. 52: 412-421.

36. Mandal, A.K. 2016. Mapping and characterization of salt-affected and waterlogged soils in the Gangetic plain of central Haryana (India) for reclamation and management. Cogent Geoscience. 2:1, 1213689, DOI: 10.1080/23312041.2016.1213689

37. Zurqani, H., Mikhailova, E., Post, C., Schlautman, M and Sharp, J. 2018. Predicting the Classes and Distribution of Salt-Affected Soils in Northwest Libya. Communications in Soil Science and Plant Analysis. DOI: 10.1080/00103624.2018.1432637

38. Ghosh, G., Kumar, S and Saha, S.K. 2012. Hyperspectral satellite data in mapping salt-affected soils using linear spectral unmixing analysis. *J Indian Soc Remote Sens*. 40:129–136.

39. Wang, L., Zhang, B., Shen, Q., Yao, Y., Zhang, S., Wei, H., Yao, R and Zhang, Y. 2021. Estimation of Soil Salt and Ion Contents Based on Hyperspectral Remote Sensing Data: A Case Study of Baidunzi Basin, China. Water.13(559). https://doi.org/10.3390/ w13040559

40. Naresh, G.D., Jayasree, G and Ramana, K.V. 2018. Characterisation and mapping of salt-affected soils in parts of Nalgonda district using hyperspectral data. International Journal Pure Applied Bioscience. 6 (6): 699-707.

41. Mashimbye, Z.E., Cho M.A., Nell, J.P., DeClercq, W.P., Van-Niekerk, A and Turner, D.P. 2012. Model-based integrated methods for quantitative estimation of soil salinity from hyperspectral remote sensing data: A case study of selected South African soils. *Pedosphere*. 22 (5): 640-649.

42. Farifteh, J., Van Der Meer, F., Atzberger, C and Carranza, E.J.M. 2007. Quantitative analysis of salt-affected soil reflectance spectra: A comparison of two adaptive methods (PLSR and ANN). Remote Sensing Environment. 110: 59-78.